(Cheng et al., 2011; Phillips et al., 2008) and are considered to be a precursor to the characteristic Lewy bodies found in surviving mDA neurons in brains from patients with PD (Fornai et al., 2004). The presence of these neuronal inclusions suggests decreased function of the ubiquitin-proteasome pathway due to the loss of normal Parkin function. However, the dependence of the phenotype on progerin expression suggests that age-related factors contribute to this dysfunction.

Our in vivo results corroborate the in vitro data that the age of iPSC-mDA neurons is reset to a "young" state not conducive to modeling late-onset features of PD. In contrast, progerin-induced neuronal aging reveals phenotypes consistent with normal aging as well as disease-associated phenotypes that reflect the synergistic interaction of genotype and age in modeling late-onset degenerative aspects of PD.

DISCUSSION

The ability to measure and manipulate age in cells differentiated from iPSCs represents a fundamental challenge in pluripotent stem cell research that remains unresolved to date. There has been considerable progress in directing cell fate into the various derivatives of all three germ layers; however, there has been no technology to switch the age of a given cell type on demand from embryonic to neonatal, adult, or aged status. This remains a major impediment in the field as illustrated by the persistent failure to generate hiPSC-derived adult-like hematopoietic stem cells, fully functional cardiomyocytes, or mature pancreatic islets, and the general inability to derive aged cell types stage appropriate for modeling late-onset diseases.

The current study represents an attempt at addressing these challenges. We define a set of cellular markers that correlates with the chronological age of donor fibroblasts, including markers of nuclear organization, heterochromatin, DNA damage, and mitochondrial stress. We demonstrate a loss of these age-associated markers upon reprogramming and report that iPSC-derived lineages do not reacquire aging features upon differentiation. We further show that in apparently healthy, non-HGPS cells, progerin exposure is sufficient to induce the same set of age-associated markers that defines the original old donor fibroblast population prior to iPSC induction. Importantly, we present an induced aging strategy that mimics several aspects of normal aging in iPSC-derived lineages beyond fibroblasts and demonstrate the utility of our approach for modeling late-onset disorders such as PD (Figure S7; Table S4).

A critical requirement for our study was the identification of markers that predict fibroblast donor age and that can be used to monitor cellular age during reprogramming, differentiation, and induced aging. In contrast to previous studies by Agarwal et al. (2010), Marion et al. (2009), Prigione et al. (2010), and Suhr et al. (2010), it was important to look at a broad set of age-related markers and to compare cellular age in matched cell fates (donor fibroblast versus iPSC-fibroblast). Future studies may include additional candidate markers such as methylation levels at particular CpG sites that have been reported to predict donor age across multiple tissues (Hannum et al., 2013; Koch and Wagner, 2011) or methylation patterns reported to reflect epigenetic memory in iPSCs of donor cell fate (Kim et al., 2010; Polo et al., 2010). It will also be interesting to include additional fibroblast lines covering the age spectrum at even higher resolution and to define whether age-related marker expression increases gradually or occurs as a binary "off/on" switch between young and old age.

One interesting aspect of our approach is the ability to induce cell-type-specific responses (Table S4). Progerin exposure can not only reestablish age in fibroblasts but also phenocopies aspects of normal neuronal aging, including the presence of neuromelanin in grafted mDA neurons, global transcriptional changes in mDA neurons after progerin exposure, and progerin-induced in vitro dendrite degeneration phenotypes. Furthermore, our results indicate that progerin levels may affect the timing by which age-related phenotypes appear. The use of modified-RNAs rapidly induced very high levels of expression and triggered age-related marker expression within just 3 days in fibroblasts and 5 days in neurons. In contrast, lentiviral expression under control of a neuronal-specific promoter led to much lower levels of expression that did not trigger an obvious phenotype at 1 month after transplantation (data not shown) but induced robust and progressive phenotypes at 3 and 6 months postgrafting. Progerin-induced age-related phenotypes occur much more rapidly than during normal aging, making induced aging an attractive yet artificial strategy for modeling late-onset pathology.

It is worth noting that progerin expression using modified-RNAs or expression under a neuron-specific promoter bypasses the differential progerin levels found across various tissues in patients with HGPS. Tissue-specific expression of A-type lamins is likely the reason why the disease does not affect all organ systems equally (Röber et al., 1989). In particular, the CNS is thought to be relatively protected due to the expression of miR-9, which targets lamin A and progerin, but not lamin C (Nissan et al., 2012). Therefore, HGPS iPSC-derived neurons are likely not a suitable alternative to the use of progerin modified-RNA to trigger in vitro neuronal aging.

Although progerin exposure may not capture all aspects of normal aging, our study demonstrates that the induced aging strategy triggers an aged-like state suitable for modeling late-onset diseases such as PD in a manner we have not known to be previously possible in the iPSC field. We observed a robust degenerative phenotype in two genetic PD iPSC models. In future studies, it will be interesting to mechanistically dissect the separate contribution of genetic and age-related disease susceptibilities such as the differences observed in grafted PINK1 versus Parkin mutant iPSC-mDA neurons using isogenic,

Dotted line indicates an equal amount of phospho protein in both treatment conditions. Quantification represents three independent cell isolates for each genotype.

*$p < 0.05$, **$p < 0.01$, and ***$p < 0.001$, according to one-way ANOVA with Dunnett's tests ($n = 3$ independent differentiations and modified-RNA transfections in all cases). Bar graphs represent mean ± SEM. +n, nuclear-GFP; +p, GFP-progerin; C1–C4, lines derived from apparently healthy donors; (R), iPSC derived using retroviral factors; (S), iPSC derived using Sendai viral factors. Scale bars, 25 μm.

See also Figures S5 and S7, and Tables S2 and S5.

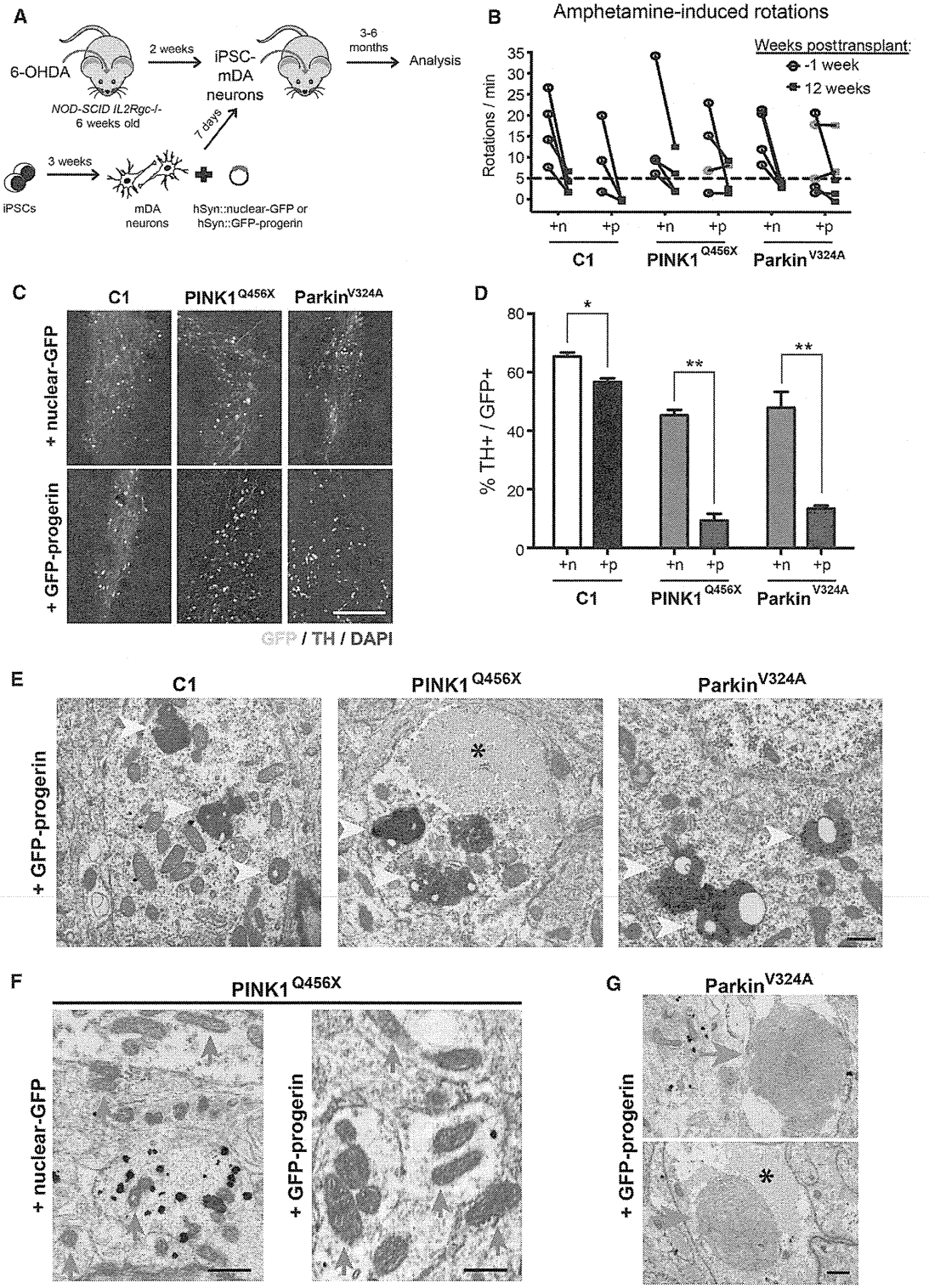

Figure 7. Long-Term Progerin Overexpression In Vivo Reveals a Severe Degenerative Phenotype in PD Mutant Cells

(A) Schematic illustration represents the transplantation studies into 6-OHDA-lesioned Parkinsonian mice.

(B) Rotational behavior analysis of lesioned mice transplanted with control or PD mutant iPSC-mDA neurons expressing *hSyn::nuclear-GFP* or *hSyn::GFP-progerin* is shown. Mice were lesioned and tested for amphetamine-induced rotation behavior twice prior to grafting. Dotted line indicates threshold for successful lesioning. Pink symbols identify successfully lesioned animals that did not show recovery (n = 3–5 animals per treatment group).

(legend continued on next page)

gene-corrected lines. Similarly, it will be important to perform time course studies to further examine the progressive reduction in TH^+ neurons upon long-term exposure in vivo despite our preliminary observations that there are comparable TH^+ neuron numbers at early time points after grafting. The ultrastructural inclusions observed in Parkin-derived mDA neurons in vivo are compatible with precursor lesions to Lewy body formation. Because Lewy bodies are less frequently observed in patients with PD with Parkin or PINK1 mutations (Nuytemans et al., 2010), it will be intriguing to test our strategy in additional PD subpopulations such as patients with mutations in α-synuclein or LRRK2 or in sporadic PD. Finally, our technology could be integrated into a drug discovery pipeline aimed at counteracting the increased disease susceptibility of aged cells, a target that cannot be pursued using current PD iPSC models where the symptom-relevant cells appear "young" and resistant to the degenerative aspect of the disease.

Our work will likely stimulate studies aimed at testing alternative and complementary "induced aging" strategies for modeling late-onset disease. It will also be important to better address the timeline and reversibility of induced aging in iPSC-derived lineages. Furthermore, it will be interesting to test whether expression of progerin at lower levels could facilitate maturation of differentiated iPSC lineages, another key bottleneck in the field. We propose induced aging as a strategy complementary to iPSC technology that may ultimately enable the precise programming of both cell fate and age on demand.

EXPERIMENTAL PROCEDURES

iPSC Derivation and Differentiation

Apparently healthy young donor, old donor, and HGPS patient and Parkinson's patient fibroblasts purchased from Coriell were reprogrammed as described (Fusaki et al., 2009) using CytoTune Sendai viruses (Life Technologies) at an MOI of ten. iPSC clones were isolated approximately 4 weeks after transduction and maintained on MEFs with weekly passaging using Dispase (STEMCELL Technologies). For differentiation, iPSCs were harvested using Accutase (Innovative Cell Technology). Fibroblast (Park et al., 2008) and mDA neuron differentiations (Kriks et al., 2011) were performed as previously described.

Modified-RNA Synthesis

Modified-RNA was generated using an in vitro transcription (IVT) protocol described previously (Mandal and Rossi, 2013; Warren et al., 2010). Transfections were performed using Lipofectamine RNAiMAX (Life Technologies) in cell-type-specific medium following treatment with an interferon inhibitor (B18R; eBioscience).

Immunocytochemical Analyses

Cell cultures were fixed in 4% paraformaldehyde. A list of antibodies and concentrations is provided in Table S5. Secondary antibodies were species-specific Alexa dye conjugates (Molecular Probes). Additional details for mouse tissue and quantification methods are described in the Supplemental Experimental Procedures. Animal procedures were performed following NIH guidelines and were approved by the local Institutional Animal Care and Use Committee (IACUC).

Flow Cytometry and mtROS Analyses

Cells were dissociated with Accutase and stained with directly conjugated antibodies (BD Biosciences). For mtROS assessment, cells were stained with MitoSOX Red (Life Technologies) at a final concentration of 20 μM in cell culture medium. Cell sorting was performed on a FACSAria (BD Biosciences).

Gene Expression Analysis

Cells were lysed with TRIzol (Life Technologies). RNA was extracted using the RNeasy kit (QIAGEN) and reverse transcribed using the SuperScript kit (Life Technologies) according to the manufacturer's instructions. Quantitative RT-PCR was performed using the Mastercycler RealPlex2 (Eppendorf) platform. For RNA-seq, total RNA was isolated from two independent experiments and processed by the MSKCC genomics core laboratory.

Protein Analysis

Cell pellets were lysed with RIPA buffer with 1% SDS. A total of 20–40 μg samples were further diluted with 4× Laemmli sample buffer, boiled for 5 min at 95°C, and loaded onto a NuPAGE 4%–12% Bis-Tris precast gel (Life Technologies). PVDF membranes were incubated in primary antibodies overnight (see Table S5 for a list of antibodies used) followed by appropriate HRP-labeled secondary antibodies (Jackson ImmunoResearch).

Xenografts

iPSC-mDA neurons were transplanted into the striatum of lesioned *NOD-SCID IL2Rgc* null mice (Jackson Laboratory) following in vitro transduction with either *hSyn::GFP-progerin* or *hSyn::nuclear-GFP* lentivirus. Immunohistochemistry of the grafts was quantified by stereological analyses. Electron microscopy was performed 6 months following transplantation as described (Milner et al., 2011).

Statistical Analyses

Distributions were compared by statistical analysis of corresponding cumulative distributions using Kolmogorov-Smirnov tests to analyze the difference between different ages or treatments. Bar graphs are plotted as mean ± SEM and represent three independent biological replicates except where noted. Two-group comparisons were analyzed using Student's t tests. Multiple-group comparisons against a control were analyzed using an ANOVA with Dunnett's test. Prism (version 6.0a; GraphPad) was used for data presentation and analysis.

ACCESSION NUMBERS

The RNA-seq data are available at Gene Expression Omnibus (http://www.ncbi.nlm.nih.gov/geo) under the accession number GSE52431.

SUPPLEMENTAL INFORMATION

Supplemental Information includes Supplemental Experimental Procedures, seven figures, and five tables and can be found with this article online at http://dx.doi.org/10.1016/j.stem.2013.11.006.

(C) Assessment at 3 months posttransplant revealed a dramatic loss of TH^+ mDA neurons in PD mutants overexpressing progerin. Scale bar, 200 μm.
(D) Quantification of the percentage of GFP+ cells that are TH^+ is shown. Data are presented as mean ± SEM (n = 3 mice per condition). *$p < 0.05$ and **$p < 0.01$, according to Student's t tests.
(E–G) Ultrastructural analysis 6 months after transplantation revealed accumulation of neuromelanin with lipofuscin deposits (E, yellow arrowheads) in grafts with progerin overexpression. Strikingly, the PINK1 mutant graft with progerin displayed enlarged mitochondria (F, compare representative mitochondria indicated by orange arrows in +nuclear-GFP and +GFP-progerin groups), whereas the Parkin mutant graft with progerin had large multilamellar bodies (G, pink arrows). These phenotypes were not observed in any other treatment groups. Asterisks in (E) and (G) indicate a fibrillar body of degenerating microtubules. Scale bars, 500 nm. Bar graph represents mean ± SEM.
See also Figures S6 and S7, and Tables S2, S4, and S5.

AUTHOR CONTRIBUTIONS

J.D.M. is responsible for the conception and study design and the reprogramming/maintenance/directed differentiation of iPSCs, cellular/molecular assays, histological analyses, data analysis and interpretation, and writing of the manuscript. Y.M.G. performed mouse transplantation and behavioral analyses. S.K. conducted mDA neuron-associated assay development and data interpretation. B.L. performed western blot analysis and data interpretation. R.L.B. is responsible for the RNA-seq analysis and data interpretation. E.Y.T. conducted flow cytometry analysis. P.K.M. provided modified-RNA cloning and technical advice. E.V. is responsible for telomere length analysis. J.-w.S. and S.K. provided mDA differentiation technical advice. T.T. performed intracellular dopamine analysis. N.F. provided the Sendai virus. M.J.T. provided technical advice and data interpretation. D.K. is responsible for the derivation of PD iPSC lines and data interpretation. T.A.M. performed electron microscopy and data interpretation. D.J.R. provided modified-mRNAs and data interpretation. L.S. is responsible for the conception and study design, data analysis and interpretation, and writing of the manuscript.

ACKNOWLEDGMENTS

We thank the K. Eggan lab for retroviral-derived control iPSCs, Philip Manos for modified-RNA technical advice, C. Klein for PD fibroblasts, Yvonne Mica and Elizabeth Calder for general technical advice and data interpretation, Andreina Gonzalez, Tracey Van Kempen, and Vladimir Mudragel for help in preparing electron microscopy samples, the MSKCC genomics core laboratory for RNA-seq, MSKCC Molecular Cytology Core facility for histology slices, and MSKCC Cytogenetics core facility for karyotyping. D.J.R. is a New York Stem Cell Foundation Robertson Investigator. The work was supported in part by Phil and Marcia Rothblum foundation by NINDS contract NS078338 and by a grant from the Tri-Institutional Stem Cell Initiative (Starr Foundation) to L.S., and NIH grants DA08259 and HL098351 to T.A.M. and NS076054 to D.K. J.D.M was supported by an NSF fellowship.

Received: August 21, 2013
Revised: September 27, 2013
Accepted: November 5, 2013
Published: December 5, 2013

REFERENCES

Agarwal, S., Loh, Y.H., Mcloughlin, E.M., Huang, J., Park, I.H., Miller, J.D., Huo, H., Okuka, M., Dos Reis, R.M., Loewer, S., et al. (2010). Telomere elongation in induced pluripotent stem cells from dyskeratosis congenita patients. Nature *464*, 292–296.

Bellin, M., Marchetto, M.C., Gage, F.H., and Mummery, C.L. (2012). Induced pluripotent stem cells: the new patient? Nat. Rev. Mol. Cell Biol. *13*, 713–726.

Bernhardt, R. (1984). Light and electron microscopic studies of the distribution of microtubule-associated protein 2 in rat brain: a difference between dendritic and axonal cytoskeletons. J. Comp. Neurol. *226*, 203–221.

Canela, A., Vera, E., Klatt, P., and Blasco, M.A. (2007). High-throughput telomere length quantification by FISH and its application to human population studies. Proc. Natl. Acad. Sci. USA *104*, 5300–5305.

Cheng, H.C., Kim, S.R., Oo, T.F., Kareva, T., Yarygina, O., Rzhetskaya, M., Wang, C., During, M., Talloczy, Z., Tanaka, K., et al. (2011). Akt suppresses retrograde degeneration of dopaminergic axons by inhibition of macroautophagy. J. Neurosci. *31*, 2125–2135.

Constantinescu, D., Gray, H.L., Sammak, P.J., Schatten, G.P., and Csoka, A.B. (2006). Lamin A/C expression is a marker of mouse and human embryonic stem cell differentiation. Stem Cells *24*, 177–185.

Cooper, O., Seo, H., Andrabi, S., Guardia-Laguarta, C., Graziotto, J., Sundberg, M., McLean, J.R., Carrillo-Reid, L., Xie, Z., Osborn, T., et al. (2012). Pharmacological rescue of mitochondrial deficits in iPSC-derived neural cells from patients with familial Parkinson's disease. Sci. Transl. Med. *4*, 41ra90.

Dechat, T., Pfleghaar, K., Sengupta, K., Shimi, T., Shumaker, D.K., Solimando, L., and Goldman, R.D. (2008). Nuclear lamins: major factors in the structural organization and function of the nucleus and chromatin. Genes Dev. *22*, 832–853.

Dodson, M.W., and Guo, M. (2007). Pink1, Parkin, DJ-1 and mitochondrial dysfunction in Parkinson's disease. Curr. Opin. Neurobiol. *17*, 331–337.

Fornai, F., Lenzi, P., Gesi, M., Soldani, P., Ferrucci, M., Lazzeri, G., Capobianco, L., Battaglia, G., De Blasi, A., Nicoletti, F., and Paparelli, A. (2004). Methamphetamine produces neuronal inclusions in the nigrostriatal system and in PC12 cells. J. Neurochem. *88*, 114–123.

Freije, J.M., and López-Otín, C. (2012). Reprogramming aging and progeria. Curr. Opin. Cell Biol. *24*, 757–764.

Fusaki, N., Ban, H., Nishiyama, A., Saeki, K., and Hasegawa, M. (2009). Efficient induction of transgene-free human pluripotent stem cells using a vector based on Sendai virus, an RNA virus that does not integrate into the host genome. Proc. Jpn. Acad. Ser. B Phys. Biol. Sci. *85*, 348–362.

Hannum, G., Guinney, J., Zhao, L., Zhang, L., Hughes, G., Sadda, S., Klotzle, B., Bibikova, M., Fan, J.B., Gao, Y., et al. (2013). Genome-wide methylation profiles reveal quantitative views of human aging rates. Mol. Cell *49*, 359–367.

Hayflick, L. (1965). The limited in vitro lifetime of human diploid cell strains. Exp. Cell Res. *37*, 614–636.

Hennekam, R.C.M. (2006). Hutchinson-Gilford progeria syndrome: review of the phenotype. Am. J. Med. Genet. A. *140*, 2603–2624.

Hof, P.R., and Morrison, J.H. (2004). The aging brain: morphomolecular senescence of cortical circuits. Trends Neurosci. *27*, 607–613.

Isacson, O., and Deacon, T. (1997). Neural transplantation studies reveal the brain's capacity for continuous reconstruction. Trends Neurosci. *20*, 477–482.

Jaworski, T., Lechat, B., Demedts, D., Gielis, L., Devijver, H., Borghgraef, P., Duimel, H., Verheyen, F., Kügler, S., and Van Leuven, F. (2011). Dendritic degeneration, neurovascular defects, and inflammation precede neuronal loss in a mouse model for tau-mediated neurodegeneration. Am. J. Pathol. *179*, 2001–2015.

Karikó, K., Buckstein, M., Ni, H., and Weissman, D. (2005). Suppression of RNA recognition by Toll-like receptors: the impact of nucleoside modification and the evolutionary origin of RNA. Immunity *23*, 165–175.

Kim, K., Doi, A., Wen, B., Ng, K., Zhao, R., Cahan, P., Kim, J., Aryee, M.J., Ji, H., Ehrlich, L.I., et al. (2010). Epigenetic memory in induced pluripotent stem cells. Nature *467*, 285–290.

Koch, C.M., and Wagner, W. (2011). Epigenetic-aging-signature to determine age in different tissues. Aging (Albany NY) *3*, 1018–1027.

Kriks, S., Shim, J.W., Piao, J., Ganat, Y.M., Wakeman, D.R., Xie, Z., Carrillo-Reid, L., Auyeung, G., Antonacci, C., Buch, A., et al. (2011). Dopamine neurons derived from human ES cells efficiently engraft in animal models of Parkinson's disease. Nature *480*, 547–551.

Lapasset, L., Milhavet, O., Prieur, A., Besnard, E., Babled, A., Aït-Hamou, N., Leschik, J., Pellestor, F., Ramirez, J.-M., De Vos, J., et al. (2011). Rejuvenating senescent and centenarian human cells by reprogramming through the pluripotent state. Genes Dev. *25*, 2248–2253.

Liu, G.H., Barkho, B.Z., Ruiz, S., Diep, D., Qu, J., Yang, S.L., Panopoulos, A.D., Suzuki, K., Kurian, L., Walsh, C., et al. (2011). Recapitulation of premature ageing with iPSCs from Hutchinson-Gilford progeria syndrome. Nature *472*, 221–225.

Liu, G.H., Ding, Z., and Izpisua Belmonte, J.C. (2012a). iPSC technology to study human aging and aging-related disorders. Curr. Opin. Cell Biol. *24*, 765–774.

Liu, G.H., Qu, J., Suzuki, K., Nivet, E., Li, M., Montserrat, N., Yi, F., Xu, X., Ruiz, S., Zhang, W., et al. (2012b). Progressive degeneration of human neural stem cells caused by pathogenic LRRK2. Nature *491*, 603–607.

Loh, Y.H., Hartung, O., Li, H., Guo, C., Sahalie, J.M., Manos, P.D., Urbach, A., Heffner, G.C., Grskovic, M., Vigneault, F., et al. (2010). Reprogramming of T cells from human peripheral blood. Cell Stem Cell *7*, 15–19.

Lutz, W., Sanderson, W., and Scherbov, S. (2008). The coming acceleration of global population ageing. Nature *451*, 716–719.

Mahmoudi, S., and Brunet, A. (2012). Aging and reprogramming: a two-way street. Curr. Opin. Cell Biol. *24*, 744–756.

Malagelada, C., Jin, Z.H., and Greene, L.A. (2008). RTP801 is induced in Parkinson's disease and mediates neuron death by inhibiting Akt phosphorylation/activation. J. Neurosci. *28*, 14363–14371.

Mandal, P.K., and Rossi, D.J. (2013). Reprogramming human fibroblasts to pluripotency using modified mRNA. Nat. Protoc. *8*, 568–582.

Mann, D.M., and Yates, P.O. (1974). Lipoprotein pigments—their relationship to ageing in the human nervous system. II. The melanin content of pigmented nerve cells. Brain *97*, 489–498.

Marion, R.M., Strati, K., Li, H., Tejera, A., Schoeftner, S., Ortega, S., Serrano, M., and Blasco, M.A. (2009). Telomeres acquire embryonic stem cell characteristics in induced pluripotent stem cells. Cell Stem Cell *4*, 141–154.

Milner, T.A., Waters, E.M., Robinson, D.C., and Pierce, J.P. (2011). Degenerating processes identified by electron microscopic immunocytochemical methods. Methods Mol. Biol. *793*, 23–59.

Nguyen, H.N., Byers, B., Cord, B., Shcheglovitov, A., Byrne, J., Gujar, P., Kee, K., Schüle, B., Dolmetsch, R.E., Langston, W., et al. (2011). LRRK2 mutant iPSC-derived DA neurons demonstrate increased susceptibility to oxidative stress. Cell Stem Cell *8*, 267–280.

Nissan, X., Blondel, S., Navarro, C., Maury, Y., Denis, C., Girard, M., Martinat, C., De Sandre-Giovannoli, A., Levy, N., and Peschanski, M. (2012). Unique preservation of neural cells in Hutchinson-Gilford progeria syndrome is due to the expression of the neural-specific miR-9 microRNA. Cell Rep. *2*, 1–9.

Nuytemans, K., Theuns, J., Cruts, M., and Van Broeckhoven, C. (2010). Genetic etiology of Parkinson disease associated with mutations in the SNCA, PARK2, PINK1, PARK7, and LRRK2 genes: a mutation update. Hum. Mutat. *31*, 763–780.

Papapetrou, E.P., Tomishima, M.J., Chambers, S.M., Mica, Y., Reed, E., Menon, J., Tabar, V., Mo, Q., Studer, L., and Sadelain, M. (2009). Stoichiometric and temporal requirements of Oct4, Sox2, Klf4, and c-Myc expression for efficient human iPSC induction and differentiation. Proc. Natl. Acad. Sci. USA *106*, 12759–12764.

Park, I.H., Zhao, R., West, J.A., Yabuuchi, A., Huo, H., Ince, T.A., Lerou, P.H., Lensch, M.W., and Daley, G.Q. (2008). Reprogramming of human somatic cells to pluripotency with defined factors. Nature *451*, 141–146.

Phillips, S.E., Woodruff, E.A., 3rd, Liang, P., Patten, M., and Broadie, K. (2008). Neuronal loss of Drosophila NPC1a causes cholesterol aggregation and age-progressive neurodegeneration. J. Neurosci. *28*, 6569–6582.

Polo, J.M., Liu, S., Figueroa, M.E., Kulalert, W., Eminli, S., Tan, K.Y., Apostolou, E., Stadtfeld, M., Li, Y., Shioda, T., et al. (2010). Cell type of origin influences the molecular and functional properties of mouse induced pluripotent stem cells. Nat. Biotechnol. *28*, 848–855.

Prigione, A., Fauler, B., Lurz, R., Lehrach, H., and Adjaye, J. (2010). The senescence-related mitochondrial/oxidative stress pathway is repressed in human induced pluripotent stem cells. Stem Cells *28*, 721–733.

Röber, R.A., Weber, K., and Osborn, M. (1989). Differential timing of nuclear lamin A/C expression in the various organs of the mouse embryo and the young animal: a developmental study. Development *105*, 365–378.

Saha, K., and Jaenisch, R. (2009). Technical challenges in using human induced pluripotent stem cells to model disease. Cell Stem Cell *5*, 584–595.

Scaffidi, P., and Misteli, T. (2005). Reversal of the cellular phenotype in the premature aging disease Hutchinson-Gilford progeria syndrome. Nat. Med. *440*, 440–445.

Scaffidi, P., and Misteli, T. (2006). Lamin A-dependent nuclear defects in human aging. Science *312*, 1059–1063.

Seibler, P., Graziotto, J., Jeong, H., Simunovic, F., Klein, C., and Krainc, D. (2011). Mitochondrial Parkin recruitment is impaired in neurons derived from mutant PINK1 induced pluripotent stem cells. J. Neurosci. *31*, 5970–5976.

Shimura, H., Hattori, N., Kubo, Si., Mizuno, Y., Asakawa, S., Minoshima, S., Shimizu, N., Iwai, K., Chiba, T., Tanaka, K., and Suzuki, T. (2000). Familial Parkinson disease gene product, parkin, is a ubiquitin-protein ligase. Nat. Genet. *25*, 302–305.

Suhr, S.T., Chang, E.A., Tjong, J., Alcasid, N., Perkins, G.A., Goissis, M.D., Ellisman, M.H., Perez, G.I., and Cibelli, J.B. (2010). Mitochondrial rejuvenation after induced pluripotency. PLoS One *5*, e14095.

Sulzer, D., Mosharov, E., Talloczy, Z., Zucca, F.A., Simon, J.D., and Zecca, L. (2008). Neuronal pigmented autophagic vacuoles: lipofuscin, neuromelanin, and ceroid as macroautophagic responses during aging and disease. J. Neurochem. *106*, 24–36.

Tain, L.S., Mortiboys, H., Tao, R.N., Ziviani, E., Bandmann, O., and Whitworth, A.J. (2009). Rapamycin activation of 4E-BP prevents parkinsonian dopaminergic neuron loss. Nat. Neurosci. *12*, 1129–1135.

Timmons, S., Coakley, M.F., Moloney, A.M., and O' Neill, C. (2009). Akt signal transduction dysfunction in Parkinson's disease. Neurosci. Lett. *467*, 30–35.

Verlinden, J., van Leuven, F., Cassiman, J.J., and van den Berghe, H. (1981). Identification of the human fibroblast surface glycoprotein (FSH) as aminopeptidase M. FEBS Lett. *123*, 287–290.

Warren, L., Manos, P.D., Ahfeldt, T., Loh, Y.H., Li, H., Lau, F., Ebina, W., Mandal, P.K., Smith, Z.D., Meissner, A., et al. (2010). Highly efficient reprogramming to pluripotency and directed differentiation of human cells with synthetic modified mRNA. Cell Stem Cell *7*, 618–630.

Wood, S.H., Craig, T., Li, Y., Merry, B., and de Magalhães, J.P. (2013). Whole transcriptome sequencing of the aging rat brain reveals dynamic RNA changes in the dark matter of the genome. Age (Dordr.) *35*, 763–776.

Zhang, J., Lian, Q., Zhu, G., Zhou, F., Sui, L., Tan, C., Mutalif, R.A., Navasankari, R., Zhang, Y., Tse, H.-F., et al. (2011). A human iPSC model of Hutchinson Gilford progeria reveals vascular smooth muscle and mesenchymal stem cell defects. Cell Stem Cell *8*, 31–45.

Stem Cell Rev and Rep (2013) 9:422–434
DOI 10.1007/s12015-012-9388-1

Mesodermal and Hematopoietic Differentiation from ES and iPS Cells

Tomoko Inoue-Yokoo · Kenzaburo Tani · Daisuke Sugiyama

Published online: 9 June 2012

Abstract Embryonic stem (ES) and induced pluripotent stem (iPS) cells can differentiate into any type of tissue when grown in a suitable culture environment and are considered valuable tools for regenerative medicine. In the field of hematology, generation of hematopoietic stem cells (HSCs) and mature hematopoietic cells (HCs) from ES and iPS cells through mesodermal cells, the ancestors of HCs, can facilitate transplantation and transfusion therapy. Several studies report generation of functional HCs from both mouse and human ES and iPS cells. This approach will likely be applied to individual patient-derived iPS cells for regenerative medicine approaches and drug screening in the future. Here, we summarize current studies of HC-generation from ES and iPS cells.

Keywords Mesoderm induction · Hematopoietic cell differentiation · ES cell · iPS cell

Abbreviations

ES	Embryonic stem
iPS	Induced pluripotent stem
HSC	Hematopoietic stem cell
HPC	Hematopoietic progenitor cell
HC	Hematopoietic cell

T. Inoue-Yokoo · D. Sugiyama (✉)
Division of Hematopoietic Stem Cells, Advanced Medical Initiatives, Department of Advanced Medical Initiatives, Kyushu University Faculty of Medical Sciences, Fukuoka 812-8582, Japan
e-mail: ds-mons@yb3.so-net.ne.jp

T. Inoue-Yokoo
Department of Medicine and Biosystemic Science, Kyushu University Graduate School of Medical Sciences, Fukuoka 812-8582, Japan

K. Tani
Department of Medical Genomics, Medical Institute of Bioregulation, Kyushu University, Fukuoka 812-8582, Japan

Introduction

Hematopoiesis is the process by which mature and functional hematopoietic cells (HCs), such as leukocytes (granulocytes, macrophages, lymphocytes), erythrocytes and platelets, are generated from hematopoietic stem cells (HSCs) and hematopoietic progenitor cells (HPCs) to maintain homeostasis. Hematopoiesis is controlled intrinsically via transcription factors and small RNAs [1–3] and extrinsically through growth factors and extracellular matrices secreted from niche cells surrounding HCs [4–6]. Faulty regulation of hematopoiesis leads to hematological diseases, such as anemia, leukemia and lymphoma, in which HSC transplantation and/or transfusion of erythrocytes or platelets are dependent on disease status. Regardless of the HSC source (patient cells, donor cells, or cord blood cells), transplantation is a promising therapy for some hematological diseases. However, problems remain in HSC transplantation, such as donor shortages, viral contamination and graft-versus host disease. To overcome these problems, HSC generation from other cells is a possible alternative to expansion of cord blood HSCs. Mature HCs, such as erythrocytes and platelets, are obtained primarily from donors and transfused into patients with hematological diseases and under surgical operation. Likewise, use of HSCs is also associated with problems, such as shortage of donors, viral infection and rejection. Overall, the ability to generate mature HCs from other cells would guarantee a continuous supply of cells and ensure safe and efficient transfusion therapy.

To address these issues, in vitro HC generation from other cells, particularly from embryonic stem (ES) cells [7] and induced pluripotent stem (iPS) cells [8], has been attempted. ES cells are established from the inner cell mass of a blastocyst, maintain their pluripotent and undifferentiated status in vitro and differentiate into any cell type in appropriate culture conditions. Furthermore, ES cells can have pluripotency in vivo and form teratoma in immunodeficient mice, and can be used to generate chimeric mice in vivo. To understand molecular mechanisms underlying developmental processes, ES cells are frequently utilized, since they mimic in vivo development in vitro (Fig. 1). iPS cells, on the other hand are created by ectopic expression of four transcription factors (Oct3/4, Sox2, Klf4, and c-Myc) in somatic cells, such as fibroblasts, hepatocytes, gastric epithelial cells, pancreatic cells, B cells and $CD34^+$ cord blood cells, and exhibit properties of pluripotent ES cells. iPS cells established from a patient's somatic cells could function as useful tools for regenerative medicine and drug screening by manipulating lineage specific differentiation in vitro (Fig. 1).

Here we summarize current studies relevant to generation of HCs and mesodermal cells from ES and iPS cells in both mice and humans (Table 1).

General Induction Methods

Several methods to differentiate mesodermal cells and hematopoietic cells from ES and iPS cells have been reported. They include (i) embryoid body (EB) formation, (ii) co-culture with feeder cells, and (iii) growth in extra cellular matrix-coated dishes. In the first method, undifferentiated ES and iPS cell colonies are separated into small cell pieces enzymatically or by physical dissection, following by EB formation in suspension in a culture dish or hanging drop. EBs are spherical cell aggregates that proliferate and differentiate into all three germ layers (i). Alternatively, ES or iPS cells can be seeded on OP9 stromal cells, which are established from the newborn calvaria of op-/op- mice and support HCs differentiation (ii), or seeded on collagen IV-coated dishes, which promote cell proliferation and form

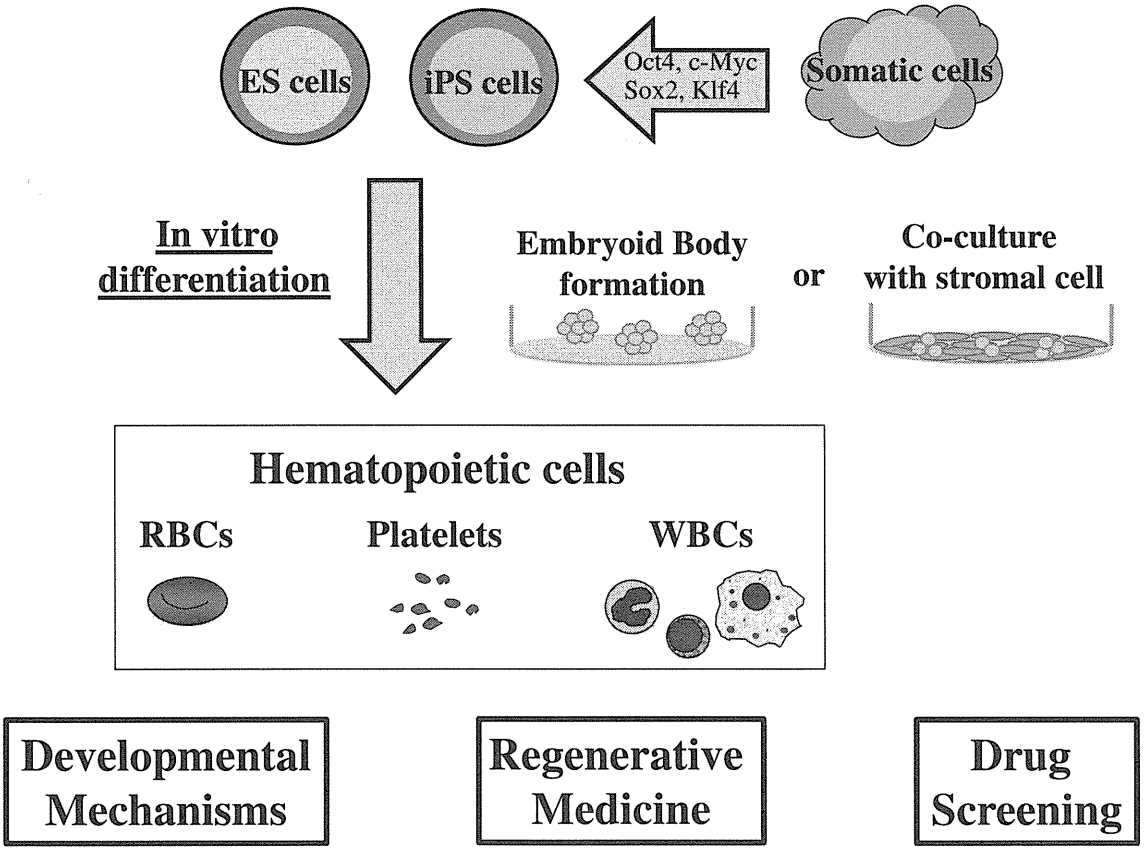

Fig. 1 Generation of hematopoietic cells from pluripotent stem cells in vitro. Embryonic stem (ES) and induced pluripotent stem (iPS) cells have been differentiated into hematopoietic cells (HCs) through mesodermal cells, ancestors of HCs, by two methods: embryoid body (EB) formation and co-culture with stromal cells in vitro. These cells are potentially applicable to regenerative medicine and drug screening by manipulating their lineage specific differentiation in vitro

Table 1 Generation of hematopoietic lineage from pluripotent stem cells

Species	Mouse		Human	
Pluripotent stem cell	ES	iPS	ES	iPS
Mesoderm	12–14	15, 16	17–20	17–20
HPC, HSC	21–23	25, 26	17, 20, 27	17, 20
Erythroid cell	28–32	25	33, 34	17-19, 35–37
Megakaryocyte	38, 39	–	41–43	44
Platelet	40	–	43	44
Macrophage	28, 43–47	48	17, 19, 35, 41	17, 19, 35
Neutrophil	49	–	18, 50, 51	52, 53
Lymphocyte	28, 54, 58, 59, 65	55, 60, 66	56, 61-63, 67	55, 67

an attachment scaffold (iii). In all cases, cell fate, directivity differentiation pattern for mesoderm and HCs differentiation is controlled by cytokines.

Mesodermal Cells

HCs are mesodermal in origin. In mammalian embryogenesis, the three germ layers, ectoderm, endoderm and mesoderm, are formed via spatiotemporal signals. Formation of the primitive streak (PS), the structure that establishes bilateral symmetry, marks the beginning of gastrulation and the emergence of mesodermal precursors. Mesoderm, derived from interaction between the endoderm and ectoderm, forms paraxial, intermediate, and lateral tissues during the mid- to late-streak stage. Among precursors in the axial, paraxial, intermediate and lateral mesoderm, blood vessels and HCs are generated from the lateral mesoderm. Therefore, the appearance of lateral mesoderm is one of indicator to hematopoietic differentiation.

One question is whether ES and iPS cell-derived cells express the surface antigen markers, such as E-cadherin (E-cad), a marker of both ectoderm and endoderm), platelet-derived endothelial growth factor receptor (PDGFRα), and Flk1 (also known as VEGF receptor 2 and a marker lateral mesoderm) [9–11] and transcription factors, such as *Tbx6* and *Brachyury* (a marker pan mesoderm) (Fig. 2).

In mouse, a high percentage of $Flk1^+$ mesodermal cells are reportedly obtained from EBs around days 4 to 4.5 after ES cell differentiation [12, 13]. ES cells cultured on collagen-IV-coated dishes differentiate into $Flk1^+PDGFR\alpha^+$ immature mesodermal precursors, which then give rise to $Flk1^+PDGFR\alpha^-$ cells, which are precursor of endothelial and HCs [14]. $Flk1^+$ mesodermal cells have been generated from several kinds of mouse iPS cells, such as mouse embryonic fibroblasts (MEFs), tail tip fibroblasts (TTFs), hepatocytes, and gastric epithelial cells. Among them, MEF-derived iPS cells exhibit the highest proportion of $E\text{-}cad^-Flk1^+$ cells [15]. Mesodermal potential as evaluated by the presence of $E\text{-}cad^-Flk1^+$ cells and expression of *Brachyury, Flk1*, and *Tbx6* mRNA vary among several iPS cell lines derived from identical TTFs. The level of ectopically expressed and remain of c-Myc likely underlies the differences [16].

Some groups have reported mesodermal differentiation from both human ES and iPS cells. $Flk1^+CD34^+$ mesodermal progenitors were generated from KhES1, KhES3 ES cells (KhES1, KhES3) and iPS cells (201B7, 253 G4; derived from dermal fibroblasts) co-cultured with OP9 cells and cytokines [17]. Morishima et al. report that ES (KhES3) and iPS (201B6, 253 G1, 253 G4; derived from dermal fibroblasts) cells generated $Flk1^+$ cells that contained hemangioblasts and $Flk1^{high}CD34^+$ cells with hematopoietic potential [18]. *BRACHYURY* and *WNT3A* mRNA expression was also confirmed in ES-, iPS-, and patient iPS-derived mesodermal cells by others [19, 20].

Hematopoietic Stem (HSCs) and Progenitor (HPCs) Cells

HSCs, which top the hematopoietic hierarchy, have self-renewal capacity and multipotency, and differentiate first into the progenitors of each hematopoietic lineage, which then mature into functional cells, including leukocytes, erythrocytes and platelets. As HSCs are used for transplantation, pluripotent cell-derived HSCs could serve as a source for future clinical applications. Questions remain as to whether HPCs and HSCs derived from pluripotent cells express c-Kit, Sca-1, CD45 in mouse, or CD34 and CD45 in humans in vitro, and whether these precursors have hematopoietic repopulation capacity in vivo (Fig. 2).

In mice, Burt et al. reported a differentiation method that did not require gene modification. EB formation of ES cells treated with SCF, IL-3 and IL-6 with serum for 7–10 days yielded $CD45^+c\text{-}Kit^+$HPCs with long term (for a maximum 20 weeks) repopulation capacity, as measured by chimerism and differentiation into lymphoid and myeloid lineages after transplantation into irradiated mice [21]. However, this approach is not widespread, suggesting that success may depend on serum they used. Therefore, establishment of serum-independent culture condition would be needed to get reproducible result.

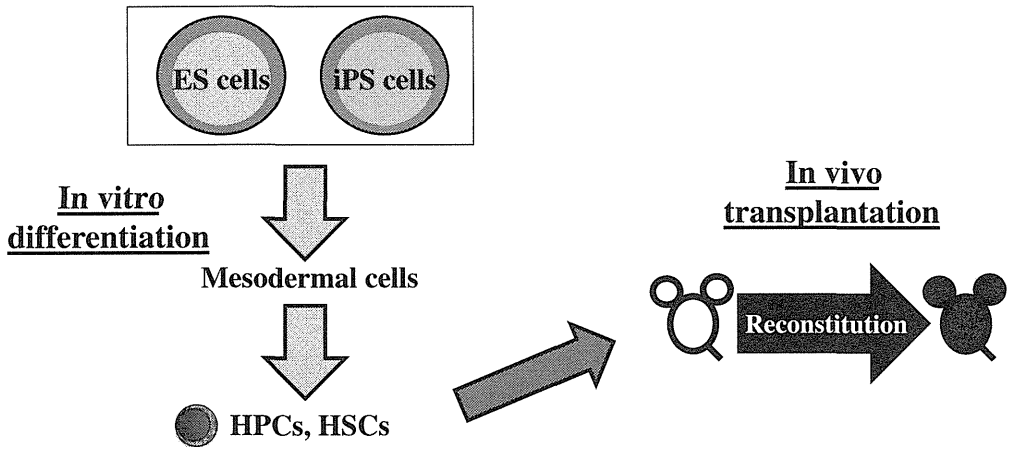

Cell types	Surface markers		Specific genes		Other characteristics
	Mouse	Human	Mouse	Human	
Mesodermal cells	FLK1		*Brachyury Tbx6*	*BRACHYURY WNT3A*	Origin of hematopoietic cells and blood vessels
HPCs HSCs	c-Kit Sca-1 CD45	CD34 CD45	*Runx1, Hoxb4, CD41, CD45*	*RUNX1, HOXB4, CD45, CD38*	Hematopoietic reconstitution capacity in transplanted mice (In vivo)

Fig. 2 Schematic diagram of pluripotent cell-derived mesodermal cells, HPCs and HSCs. ES and iPS cells- derived mesodermal cells are characterized by the expression of FLK1 (also known as VEGF receptor 2) and specific transcription factor genes (*Brachyury* and *Tbx6* in mouse; *BRACHYURY* and *WNT3A* in human). Hematopoietic progenitor cells (HPCs) and hematopoietic stem cells (HSCs)-derived from pluripotent cells are characterized by the expression of hematopoietic surface markers (c-Kit, Sca-1 and CD45 in mouse; CD34 and CD45 in human) and specific transcription factor genes (*Runx1, Hoxb4, CD41* and *CD45* in mouse; *RUNX1, HOXB4, CD45* and *CD38* in human). In vivo transplantation assay enables us to evaluate the potential of both HPCs and HSCs. Extensive long-term reconstitution with multipotency and self-renewal capacities of all hematopoietic lineages can be observed in HSCs, whereas short and/or relatively long-term reconstituting in HPCs can give rise to certain lineages

On the other hand, to promote the development and expansion of ES cell-derived HSCs, genetically-modified methods have been reported. Kyba et al. reported that forced expression of HoxB4 in immature ES cell-derived HPCs conferred definitive hematopoietic potential in mouse ES cells [22]. Temporal induction of HoxB4 during the course of EB formation increased the number of immature HPCs in vitro. In addition, HoxB4-induced ES-derived HPCs engrafted and produced lymphoid and myeloid cells in both primary (for a maximum 12 weeks) and secondary (for a maximum of 20 weeks) transplanted mice [22]. Combined ectopic expression of HoxB4 and Cdx4, which is also homeobox transcription factor, resulted in more efficient reconstitution than HoxB4 alone [23]. Unlike the case in mouse, a high incidence of leukemia occurred after transducing a *HOXB4*-expressing retroviral vector in large animals, such as dog and monkey [24], suggesting that care should be taken using gene-manipulation methods for HSC transplantation.

The HoxB4-constitutive transduction method is also effective to establish mouse iPS cells from fibroblasts in a sickle cell anemia model. Resulting iPS cell-derived progenitors grown in the presence of OP9 stromal cells reconstituted the hematopoietic system after transplantation into irradiated mice [25]. Lin et al. has reported a hematopoietic differentiation culture method for iPS cells established from MEFs, which lacks a feeder cell layer or gene manipulation. After 7 days of culture with "conditioned medium", EBs prepared from culture of OP9-DL1 cells (modified OP9 cells expressing the delta-like 1 (DL1) Notch ligand) generated c-Kit$^+$Sca1$^+$HPCs that could differentiate along the myeloid lineage [26].It has not yet been examined whether HPCs derived from this method could reconstitute in vivo.

Unlike the case in mouse, ectopic expression of HoxB4 temporarily enhanced generation and proliferation of human HPCs in vitro but did not promote a significant increase in the number of HSCs in vitro and had no effect on repopulating capacity of HSCs in immuno-deficient mice [27]. This

finding suggests that other factors regulate HSC generation from human ES cells.

Importantly, Niwa et al. report that a novel serum-free monolayer culture system, independent of OP9 feeder cells and EB formation enables hematopoietic differentiation from both ES (KhES1) and iPS (201B7, 253 G4) cells. Using the method, the investigators generated $CD34^+CD45^+$ HPCs from human KhES1 between culture days 10 to 25 [17]. Tolar et al. reported hematopoietic differentiation of iPS cells from patients with mucopolysaccharidosis (MPS) type I, which is treated via HSC transplantation. An EB-mediated method generated HPCs expressing CD34 and CD45 and HSCs expressing *CD34* and *CD38* mRNA [20]. It is now necessary to determine whether HPCs derived from gene manipulation-free methods can have repopulation capacity in vivo.

Erythroid Cells

Red blood cells (RBCs), which are differentiated from erythroid progenitors (BFU-E, CFU-E) and erythroblasts, deliver oxygen (O_2) to the body tissues. Pluripotent cell-derived erythroid cells could be utilized as blood products in future clinical applications. It is not yet known whether erythroid cells derived from ES and iPS cells are definitive (EryD), enucleate, generate adult type of hemoglobin or carry oxygen (Fig. 3). In mouse, ES-derived cells co-cultured with OP9 cells contain primitive erythroid cells (EryP) within 8 days and erythroid progenitor cells (EryD) in 10 when cultured in methylcellulose semi-solid culture in the presence of Epo and IL-3. $Ter119^+$ cells were generated in the same condition after 14 days [28–30]. Within 5–6 days, EB culture-derived cells contain erythroid progenitor cells in methylcellulose culture in the presence of Epo and SCF, and those cells show a peak of *βH1 globin*, *βmajor globin* and *Gata1* gene expression within 7–8 days of culture [31].In addition to co-culture and EB formation methods, a three-step differentiation method is highly efficient in inducing erythroid cells from ES cells [32]. After 6 days of EB culture, ES-derived erythroid cultures (ES-EPs), which contain $CD71^+$c-$Kit^+Ter119^+$proerythroblasts and *βmajor globin*-expressing definitive erythroid cells, are induced with Epo, SCF, dexamethasone (Dex), insulin-like growth factor (IGF)-1. Following that, Epo, insulin, glucocorticoid receptor antagonist and transferrin were added to induce hemoglobinized, enucleated RBCs from ES-EP cells that also differentiate into $Ter119^+$ cells in vivo [32]. Hanna's group reported that after 6 days of culture on OP9 stromal cells, mouse autologous iPS cells, which were established from fibroblasts from a sickle cell anemia model, gave rise to c-Kit^+CD41^+ early HPCs in vitro and that HPCs derived by EB formation could rescue anemia in vivo after transplantation [25]. This work suggested that similar strategies are possible in humans.

Human ES cells co-cultured with mouse fetal liver-derived stromal cells (mFLSCs) generated erythroid progenitors after day 10, dominantly express adult type β-globin rather than embryonic type ε-globin, and gradually enucleate and show oxygen saturation around day 16 [33]. Lu et al. report that functional oxygen-carrying erythrocytes can be prepared on a large scale (10^{10}–10^{11} cells per 6-well plate of human ES cells) using four culture steps. They are: Step1; EB formation and hemangioblast precursor induction with BMP4, $VEGF_{165}$, bFGF, SCF, TPO and Flt-3 L (days −3.5 to 0); Step2; hemangioblast expansion with bFGF and tPTD-HoxB4 fusion protein (days 0 to10); Step3; erythroid cell differentiation and expansion with EPO (days 11 to 20); and Step4; enrichment of erythroid cells (day21) [34]. Human fibroblast-derived cell lines, such as hFib2-iPS5, 201B6, 201B7, 253G1 and 253G4, and the bone marrow mesenchymal stem cell-derived MSC-iPS1 cell line, all established from healthy donors, produced erythroid cells at around 30 days of culture via either EB formation or co-culture with OP9 stromal cells [17–19, 35]. On the other hand, two groups reported that human iPS cells from patients with hematological diseases also differentiated into erythroid cells. A combination method using EBs and OP9 cells produced BFU-E progenitor cells from dermal fibroblast-reprogrammed iPS cell lines, which were established from patients with Fanconi anemia (FA) [36]. Human peripheral blood-reprogrammed iPS cells established from patients with polycythemia vera (PV), a myeloproliferative disorder, also differentiate into CFU-E and $CD45^-$/CD235a $(GPA)^+$ mature erythroid cells after 2–3 weeks of EB formation, followed by culture of EB-derived $CD34^+CD45^+$ cells with SCF, IL-3. EPO [37].

Megakaryocytes and Platelets

Platelets, which are derived from fragmentation of precursor megakaryocytes, play a pivotal role in hemostasis by aggregation and adhesion to subendothelial tissue. In terms of regenerative medicine, pluripotent cell-derived platelets could be utilized as blood products in clinical settings. As an experimental tool, pluripotent cell-derived megakaryocytes could be useful to explore signaling pathways utilized in platelet formation, as a genetic approach has limited utility in studying anucleated platelets. One question is whether cells derived from ES and iPS cells would express surface antigen marker, such as CD41 andCD61, have the same signal pathway, exhibit the same morphology and have the same aggregation and adhesion capacity as megakaryocytes and platelets in vivo (Fig. 4).

In mice, Era et al. first reported that megakaryocytes derived from ES cells were observed 8 days after co-culture with OP9 cells and TPO [38].Co-culture of ES cells with OP9

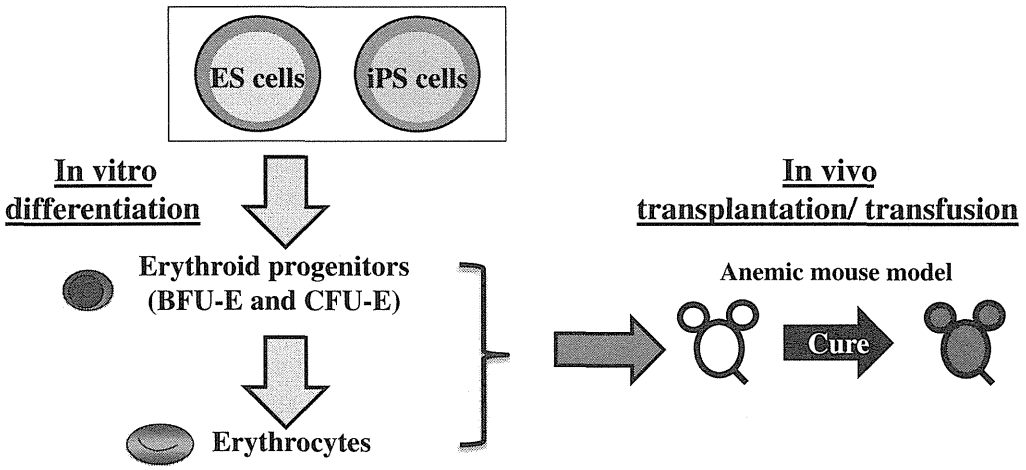

Cell type	Surface markers		Specific genes		Other characteristics
	Mouse	Human	Mouse	Human	
Erythrocytes	Ter119	GPA	*Gata1* *Eklf* *βH1–globin* *β major-globin*	*GATA1* *EKLF* *β-GLOBIN*	1) Oxygen-carrying capacity 2) Improvement the anemic status by transplantation and transfusion (In vivo)

Fig. 3 Schematic diagram of pluripotent cell- derived erythrocytes. ES and iPS cells-derived erythrocytes are characterized by the expression of erythroid surface markers (Ter119 in mouse; Glycophorin A in human) and specific transcription factor genes (*Gata1, Eklf, βH1-globin* and *β−major globin* in mouse; *GATA1, EKLF* and *β-GLOBIN* in human). Hemoglobins in erythrocytes function as an oxygen-carrier and can be evaluated by plotting the oxygen equilibrium curves. To further investigate the function of erythrocytes in vivo, erythrocytes are transplanted/transfused into anemic mouse model. BFU-E; Burst Forming Unit-Erythroid, CFU-E; Colony Forming Unit-Erythroid, GPA; Glycophorin A

stromal cells for 8–12 days in the presence of TPO, IL-6 and IL-11 resulted in development of large, polyploid megakaryocytes, which produce proplatelets, could bound fibrinogen after exposure to platelet agonists, and exhibited integrin-mediated megakaryocyte signaling [39]. Fujimoto et al. confirmed primitive and definitive megakaryopoiesis from mouse ES cells with OP9 stromal cells in the presence of TPO. At the same time, $CD41^+$ platelets were generated in the culture supernatant via two waves of differentiation. ES-derived platelets of the definitive wave are similar in structure to those in peripheral blood and exhibit fibrinogen-binding ability and CD62P (P-selectin) expression after addition of AYPGFK, a platelet agonistpeptide [40].

In humans, 17 days after human H1 ES-derived cells on mouse bone marrow S17 cell lines contained megakaryocyte progenitor cells (CFU-Mk) that expressed CD41 antigen [41]. Gaur et al. reported that human H9 ES-derived cells grown on OP9 cells also generate megakaryocytic cells after 15–17 days of culture with TPO. CD41-, CD42b- and von Willebrand factor (vWF)-expressing megakaryocytes were polyploid (2 N to 32 N) and responsive to integrin $\alpha_{IIb}\beta_3$ activation by agonists such as ADP and PAR1 [42]. Takayama et al. reported a modified method of OP9 co-culture useful to produce not only megakaryocytes but also functional platelets. Differentiated ES cells co-cultured on OP9 or 10 T1/2 cells (a mouse embryonic mesenchymal stem cell line) with VEGF for 14–15 days formed embryonic stem cell-derived sacs (ES-sacs), which consist of multiple cysts that retain properties of endothelial cells and express CD34, VE-cadherin, CD31, CD41a, and CD45. After 9–10 days culture of ES-sacs with TPO, IL-6, IL-11, SCF and heparin, cultures produced functional platelets [43]. The same group succeeded in inducing platelets through "iPS-sacs" from human iPS cell lines reprogrammed from healthy adult human dermal fibroblasts [44].

Macrophages

Macrophages, which are differentiated from monocytes, are amoeboid cells that function in both innate immunity and adaptive immunity, phagocytize bacteria, viruses and dead cells, and stimulate lymphocytes and other immune cells to respond to pathogens. Monocytes and macrophages play a critical role in initiation and progression of atherosclerotic lesions. Therefore, pluripotent cell-derived macrophages could be used in vitro as an experimental tool to clarify the mechanisms of atherosclerotic lesions. It is not known whether macrophages derived from pluripotent cells express

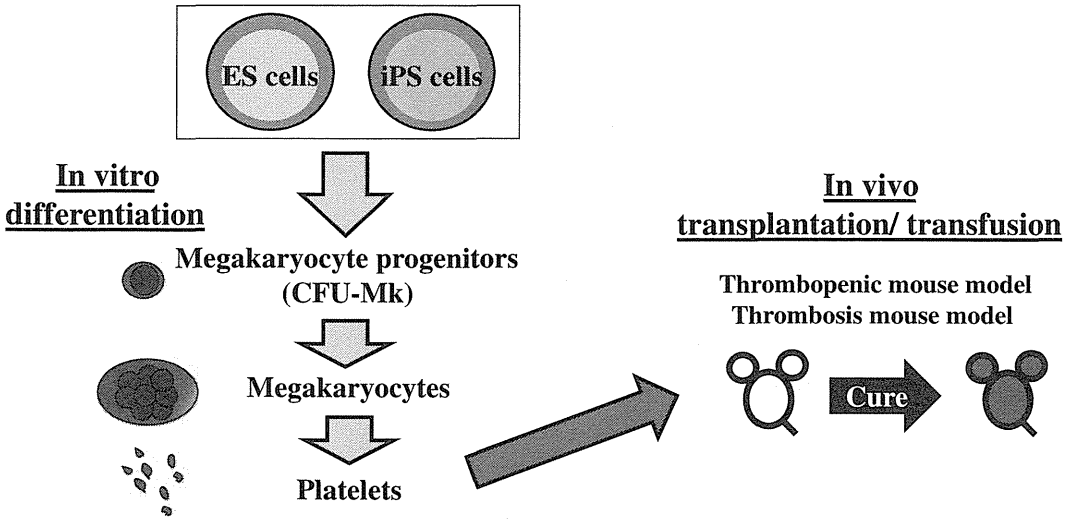

Cell types	Surface markers	Specific genes	Other characteristics
Megakaryocytes	CD41, CD42 CD61	*NF-E2* *FOG-1, Fli-1*	1) DNA ploidy 2) Aggregation and adhesion capacity
Platelets	CD41, CD42 CD61, CD62P	—	1) Aggregation and adhesion capacity 2) Thrombus formation to blood vessel injury (In vivo)

Fig. 4 Schematic diagram of pluripotent cell-derived megakaryocytes and platelets. ES and iPS cells-derived megakaryocytes are characterized by the expression of megakaryocyte surface markers (CD41, CD42 and CD61 in both mouse and human) and specific transcription factor genes (*NF-E2, FOG-1* and *Fli-1* in both mouse and human). DNA ploidy, a representative characteristic of megakaryocytes is examined in CD41 positive cells. Aggregation and adhesion capacity, another characteristic of megakaryocytes, are examined by fibrinogen binding assay and the integrin alpha II beta 3 signaling pathway. ES and iPS cells-derived platelets are characterized by the expression of surface markers (CD41, CD42, CD61 and CD62P in both mice and human). To further investigate the function of platelets in vivo, platelets are transplanted/transfused into thrombopenic mice and injury-induced mice models, in which the improvement of its status and hemostasis can be evaluated, respectively. CFU-Mk; Colony Forming Unit-Megakaryocyte

appropriate cell surface antigen markers, such as CD11b and F4/80, exhibit similar gene expression patterns as normal macrophages, or show phagocytotic activity (Fig. 5).

In mice, 13–15 days after EB formation by ES cells (CCEG2 and D3) in the presence of Epo, IL-1, IL-3, and M-CSF, HCs containing macrophages are generated [45]. Co-culture on OP9 cells with ES (D3) cells for 10 days also induced macrophage progenitors in the presence of IL-3 and Epo [28]. In these reports, macrophages were confirmed by morphologically. Lindmark et al. found that ES-derived macrophages are more similar to those in the peritoneum than mouse macrophage cell lines (J774.A1 and RAW264.7) by DNA microarray analysis [46]. After 10–12 days of culture, ES (J1) cells formed EBs in methylcellulose in the presence of CSF-1 and IL-3. After 3–5 days of liquid culture with CSF-1 and IL-3, differentiated cells expressed F4/80, FcγRII, scavenger receptor A (SR-A), CD36 and CD68, exhibited phagocytosis, and secreted TNF-α and IL-6 in response to an inflammatory stimulus [47], suggesting ES cell-derived macrophages could be an appropriate model to study atherosclerosis-related macrophages. Senju et al. reported that F4/80- and CD11b- expressing macrophages from the mouse iPS cell line 38C-2, which was established from MEFs with Oct3/4, Sox2, Klf4, and c-Myc, were generated via co-culture with OP9 cells for 6 days without cytokines and for the next 6 days with GM-CSF, followed by feeder free culture with M-CSF. iPS-derived macrophages also showed complement C5a-induced chemotaxis, phagocytic capacity and produced nitric oxide after stimulation with LPS and IFN-γ [48].

In humans, 17 days after human H1 ES-derived cells on mouse bone marrow S17 cell lines contained macrophage progenitor cells (CFU-M) that expressed CD15 antigen [35, 41]. Human ES cell lines, such as KhES-1, KhES-3, H1 and HES2, and human fibroblast-derived cell lines, such as hFib2-iPS5, 201B7 and 253G4 and the bone marrow mesenchymal stem cell-derived MSC-iPS1 line, all established from healthy donors, contained CFU-Ms and produced $CD14^+$ monocytes, $CD11b^+$ macrophages (at day14–22) and $CD13^+$ myeloid cells (at day 30) after culture via EB formation or co-culture with OP9 stromal cells in the presence of cytokines [17, 19, 35].

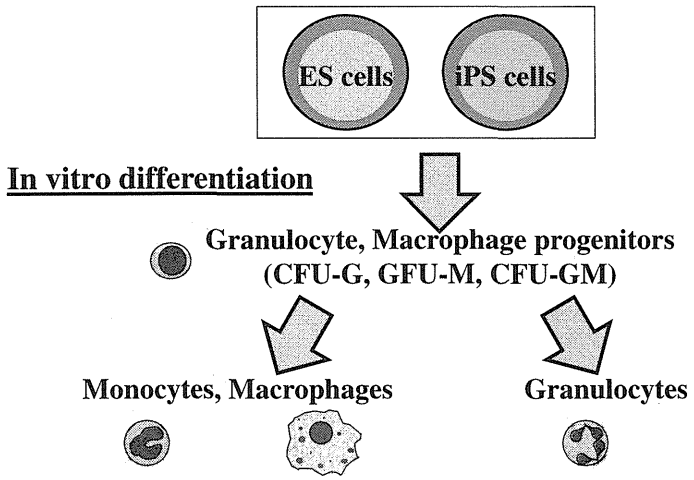

Cell types	Surface markers		Specific genes		Other characteristics
	Mouse	Human	Mouse	Human	
Monocytes Macrophages	CD11b, CD14, F4/80	CD11b, CD13, CD14, CD15, CD18	*MMP-3* *MMP-9*	*PU.1*	1) Phagocytotic capacity 2) Cytokine production
Granulocytes	Gr-1	CD11b, CD13, CD16, CD33	*PU.1*	*PU.1, MPO, CEBPα Lactoferrin Gelatinase*	1) Superoxide production 2) Chemotactic capacity

Fig. 5 Schematic diagram of pluripotent cell-derived monocytes, macrophages and granulocytes. ES and iPS cells-derived monocytes and macrophages are characterized by the expression of surface markers (CD11b, CD14 and F4/80 in mouse; CD11b, CD13, CD14, CD15 and CD18 in human) and specific transcription factor genes (*Metalloproteinase (MMP)-3* and *MMP-9* in mouse; *PU.1* in human). A representative characteristic of macrophages is phagocytotic capacity, in which fluorescence-conjugated *Escheria coli* is administered and its incorporation into macrophages is evaluated by in vitro culture. Also, macrophages can produce cytokine (interleukine-6 and tumor necrosis factor) in response to inflammatory stimulus, such as lipopolysaccharide. ES and iPS cells-derived granulocytes are characterized by the expression of surface markers (Gr-1 in mouse; CD11b, CD13, CD16 and CD33 in human) and specific transcription factor genes (*PU.1* in mouse; *PU.1, Myeloperoxidase (MPO), CEBPα, Lactoferrin* and *Gelatinase* in human). The representative characteristics of granulocytes are superoxide production in response to phorbolmyristate acetate (PMA) stimuli, and chemotactic capacity in response to the chemo-attractant in vitro. CFU-G; Colony Forming Unit-Granulocyte, CFU-M; Colony Forming Unit-Macrophage, CFU-GM; Colony Forming Unit-Granulocyte Macrophage

Granulocytes

Granulocytes, which are derived from common myeloid progenitors and myeloblasts and account for approximately 60 % of leukocytes, are composed of neutrophils, basophils and eosinophils. They contain cytoplasmic granules and play a pivotal role in immunesystem by consuming bacteria and dead cells. Decreases in the number of neutrophils promote infection in several pathological situations, such as leukocyte function deficiencies or myelosuppression caused by chemotherapy. Granulocyte transfusion therapy is considered effective for infections unresponsive to conventional antimicrobial therapies in severely neutropenic cancer patients. Therefore, pluripotent cell-derived neutrophils could be used for such procedures. Thus it is important to determine whether neutrophils derived from pluripotent cells express appropriate markers and exhibit behaviors such as chemotaxis and phagocytosis (Fig. 5).

Leiber et al. reported that mouse CCE ES cell-derived neutrophils are generated after 8 days of EB culture, followed by 7 days of co-culture with OP9 cells and cytokines. The co-culture system is more effective in enhancing the number and culture period of neutrophils produced from ES cells compared to methods that do not employ OP9 stromal cells. Those neutrophils are positive for the surface marker Gr-1, have granules containing lactoferrin and gelatinases, and exhibit chemotactic responses and superoxide production [49].

Several groups have reported neutrophil induction from human ES cells. EB formation of human KhES cells grown in the presence of OP9 cells and cytokines gives rise to CD15-, CD11b- (both neutrophil and monocyte markers) and CD16- (mature neutrophil marker) positive cells at day13 similar to neutrophils found in peripheral blood. They also exhibit the oxidative burst function in killing microorganisms and phagocytotic activity in vitro [50]. Saeki et

al. developed feeder free culture systems for neutrophil induction. ES-derived neutrophils were generated after 3 days of "sphere formation" culture of KhES-3 ES cells on low-attachment dishes in the presence of cytokines, followed by culture on gelatin-coated dishes up to 40 days, results similar to those reported by Yokoyama's group [51]. Choi et al. succeeded in expanding neutrophils from human ES cells at least 60 times more efficiently than previously reported. Their culture system employed three steps, including induction of $CD34^+/CD45^+$ HPCs for 9 days on OP9 cells, expansion of HPCs for 2–8 days without OP9 cells, and differentiation of HPCs for 8 days on OP9 cells plus G-CSF. In addition, a similar method is reportedly useful for human iPS cell lines established from neonatal foreskin and adult fibroblasts [52]. Morishima et al. analyzed the differentiation process and function of iPS-derived neutrophil in greater detail. Expression of *PU.1*, *CEBPα*, *MPO*, *lactoferrin*, and *gelatinase* was confirmed during induction, as was chemotactic activity, phagocytotic activity, and MPO chlorination activity was observed in neutrophils derived from 201B6, 253G1, 253G4 iPS cell lines, all of which were established from healthy dermal fibroblasts [18].

Recently, Zou's group reported that culture on OP9 stromal cells of human autologous iPS cells established from bone marrow mesenchymal stem cells from a patient with X-linked chronic granulomatous disease (X-CGD) gave rise to oxidase-deficient neutrophils. They were also successful in rescuing oxidase-deficiency by gene modification using zinc finger nuclease-mediated safe harbor targeting [53]. These findings demonstrate that precise gene targeting may be applied to correct a disease-causing mutation in patient iPS cells.

Lymphocytes

Lymphocytes, which consist of small lymphocytes (T cells and B cells) and large granular lymphocytes (NK cells), determine the specificity of immune response to infectious microorganisms and foreign substances. A decrease in lymphocyte number results in serious infections in several pathological situations, such as leukocyte function deficiencies or myelosuppression caused by chemotherapy. Immunotherapy for cancer is considered to be effective for cancer patients in clinical settings. Therefore, antitumor lymphocytes derived from pluripotent stem cells may be applicable to these approaches. It becomes the focus whether lymphocytes-derived from pluripotent cell express the surface antigen marker, achieve rearrangement of T cell antigen receptor (TCR) in T cell and immunoglobulin (Ig) in B cell and function such as cytotoxity (Fig. 6).

In mice, Nakano et al. reported that ES cells co-cultured on OP9 cells with IL-7 generated $B220^+$ early B cells, which were almost all IgM^- and achieved diversity-joining gene rearrangement, although a small portion of the hematopoietic cluster differentiated into mature IgM^+ cells expressing the complete μ chain mRNA [28]. B cell maturation from ES cells was enhanced in the presence of IL-7 and Flt3-L. Treatment with LPS stimulated B cell maturation and IgG secretion [54]. B cell differentiation from mouse iPS cells via the OP9 method revealed differences in outcomes according to iPS cell origin. MEF-derived iPS cells differentiated into B cells; however, B cell-derived iPS cells were relatively resistant to B cell lineage differentiation and showed defective Pax5 expression in differentiated cells [55].

Human H1 and H9 ES cell-derived $CD34^+$ cells co-cultured with MS-5 stromal cells in the presence of IL-3, IL-7, SCF and Flt3-L generated B cells positive for CD19 and for mRNA encoding the pre-B receptor complex (*VpreB*, *Igα*) [56]. Carpenter et al. first reported B cell lymphopoiesis from human iPS cells. $CD45^+CD19^+CD10^+$ cells-derived from iPS cells also expressed *Pax5*, *IL7αR*, *λ-like* and *VpreB receptor* mRNA. $CD45^+CD19^+$ cells exhibited multiple genomic D-J (H) rearrangements suggestive of pre-B-cell status [57].

T cell induction from ES cells has rarely been successful, due to difficulties in recapitulating the thymic stromal environment. de Pooter et al. reported that low population of $CD4^+$ and $CD8^+$ thymic subsets were generated from mouse ES cells as a result of co-culturing on OP9 cells, followed by $Flk1^+CD45^-$HPCs generated on fetal thymic organ cultures (FTOCs) [58]. They also developed modified OP9-DL1, which sustained mature T cells that expressed γδ and αβ TCRs, were positive for CD8, and produced IFN-γ in response to stimulation [59]. The OP9-DL1 method was also useful for mouse iPS differentiation. iPS-derived T cells secreted IL-2 and IFN-γ in response to in vitro stimulation and could also reconstitute T cell pools in Rag-deficient mice, suggesting that they follow a normal T cell differentiation program [60].

Galic et al. reported T-cell differentiation from human ES cells. Resulting differentiated H1 ES cells-derived progenitors grown in the presence of OP9 stromal cells for 10 to 19 days in vitro engrafted into human thymic tissues in immunocompromised mice. T cell development was observed in the conjoint organ 3–5 weeks after transplantation, indicating that human ES cells could be used to treat T cell disorders [61]. EB-derived T cell progenitors also generate to phenotypically and functionally normal cells of the T lineage when transferred into human thymic tissue implanted in immunodeficient mice [62]. Moreover, Timmermans et al. reported that during differentiation of ES cells on OP9 cells, two-dimensional structures form that strongly resemble blood islands, which arise during normal embryonic development and consist mostly of $CD34^+$ cells. Sequential culture of ES cell-derived cells on OP9-DL1 monolayers produced $CD34^{high}CD43^{low}$ cells that generated T cells. These hESC-derived T cells proliferated in response to

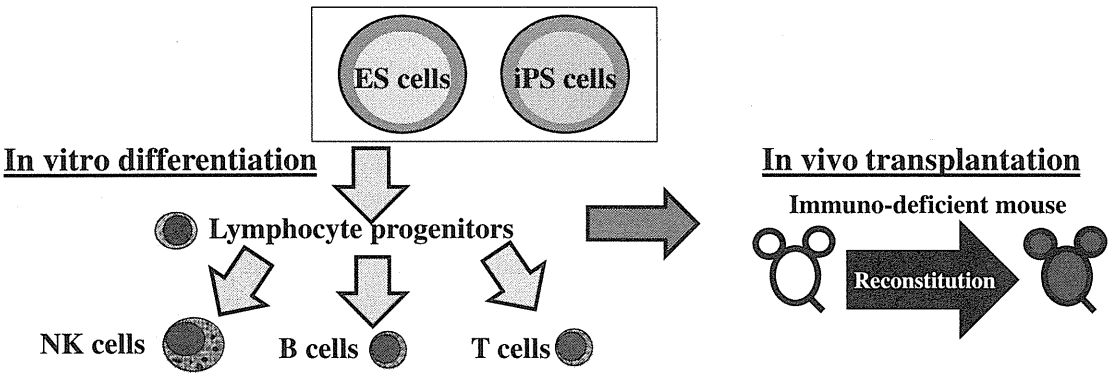

Cell types	Surface markers		Specific genes		Other characteristics
	Mouse	Human	Mouse	Human	
T cells	CD4, 8 TCR	TCR, CD3 CD4, CD7, CD8, CD45	*Rag1* *Hes1* *Gata3*	*HES1* *CD3* *GATA3*	1) Cytokine production 2) T cell differentiation in transplanted mouse (In vivo)
B cells	B220 CD19	CD10 CD19 CD45	*IgM* *Pax5*	*IgM* *PAX5* *λ-like*	1) Rearrangement of VDJ 2) Rearrangement of VJ
NK cells	CD94	CD45 CD56 CD94	*CD94, Ly49, NKR-P1, Granzyme A,B*	*CD122* *ID2* *ID3*	1) Cytotoxity 2) Cytokine production

Fig. 6 Schematic diagram of pluripotent cell-derived lymphocytes. ES and iPS cells-derived T cells are characterized by the expression of surface markers (CD4, CD8 and T cell receptor (TCR) in mouse; TCR, CD3, CD4, CD7, CD8 and CD45 in human) and specific transcription factor genes (*Rag1, Hes1* and *Gata3* in mouse; *HES1, CD3* and *GATA3* in human). A representative characteristic of T cells is cytokine (interleukin-2 and interferon-γ) production in response to anti-CD3 antibody and PMA in vitro. To further investigate the in vivo differentiation of pluripotent cells into T cells, pluripotent cells are transplanted into congenic mice in the mouse T cells and SCID-hu mice in human, respectively. ES and iPS cells-derived B cells are characterized by the expression of surface markers (B220 and CD19 in mouse; CD10, CD19 and CD45 in human) and specific transcription factor genes (*IgM* and *PAX5* in both mouse and human). A representative characteristic of B cells is VDJ and VJ gene rearrangement, which reveals early B cell commitment from pro-B cell to pre-B cells, and from pre-B cells to immature-B cells, respectively. Other characteristic of B cells is the protein expression of immunoglobulin chains such as μH chain composing pre-B receptor and L-chain for IgM, respectively. ES and iPS cells-derived NK cells are characterized by the expression of surface markers (CD94 in mouse; CD45, CD56 and CD94 in human) and specific transcription factor genes (*CD94, Ly49, NKR-P1, Granzyme A* and *Granzyme B* in mouse; *CD122, Inhibitor of DNA binding (ID) 2* and *ID3* in human). The representative characteristics of NK cells are tested by cytotoxity assay and cytokine (interleukine-6 and tumor necrosis factor alpha) production in vitro, which reveals the abilities to kill the tumor cells and to initiate the immune reaction, respectively

PHA stimulation, suggesting that hESCs can give rise to functional T cells [63]. Nevertheless, $CD34^+CD45^+$ cells from hESCs did not produce T cells on either OP9-DL1 monolayers or in FTOC cultures [64].

Mouse ES cells co-cultured with OP9 cells in the presence of Flt3-L, IL-15, IL-6, IL-7 and SCF generated NK cells, which were positive for CD94/NKG2 receptors and functioned to kill certain tumor lines and MHC class-I-deficient lymphoblasts [65]. Natural killer T (NKT) cells are a heterogeneous group of T cells that share properties of both T and NK cells. The OP9-DL1 method was also useful for NKT cell differentiation of mouse iPS cells established from MEFs and adult splenic NKT cells. iPS-derived NKT cells secreted the Th1 cytokine IFN-γ in response to in vitro stimulation and could recapitulate the adjuvant effect and suppress tumor growth in vivo [66].

Ni et al. reported NK cell generation from human H9 ES and BJ1-iPS12 iPS cells established from healthy adult human dermal fibroblasts. Among $CD45^+CD56^+$ cells generated, $CD117^-CD94^+$cells were mature NK cells with cytotoxic activity in vitro. In addition, both ES cell- and iPS cell-derived NK cells inhibited HIV-1 infection of a CEM cell line and of human primary $CD4^+$ T cells via killing through direct lysis, antibody-dependent cellular cytotoxicity, and production of chemokines and cytokines [67].

Perspective

Basic researchers have established methods for HSC and mature HC differentiation from ES and iPS cells that could

be useful for potential transplantation and transfusion therapy. Time will be required to standardize these methods, since individual researchers use diverse materials and methods, resulting in varied differentiation capability among ES and iPS cells, depending on cell line, passage number, methylation status and cell origin. To minimize clinical risks, special attention to potential tumorigenicity of manipulated cells must be paid. Although culture conditions, such as use of feeder-free cultures or serum-free media have already been improved, it remains necessary to shorten culture periods for iPS cell establishment and differentiation of the desired cell lineage induction from ES or iPS cells. Recently, "direct conversion" from human fibroblasts to HPCs and mature HCs was reported without establishing iPS cells [68]. In that case, ectopic expression of OCT4 plus treatment with a specific cytokine was effective to induce the $CD45^{+}$ cells, which had in vivo engraftment capacity. This method represents a new approach for autologous cell-transplant therapies that avoids difficulties involved with using human pluripotent stem cells. Thus, some issues remain to be resolved before ES and iPS cells can be applied to regenerative medicine.

Acknowledgments We thank Dr. Koichi Akashi, Dr. Kasem Kulkeaw, Ms. Yuka Horio, Ms. Chiyo Mizuochi, Ms. WaiFeng Lim and Dr. Elise Larmar for research support, and grant supports from the Ministry of Education, Culture, Sports, Science and Technology, the Ministry of Health, Labor and Welfare, and the Japan Society for the Promotion of Science.

Conflict of interest The authors indicate no potential conflicts of interest.

References

1. Dzierzak, E., & Speck, N. A. (2008). Of lineage and legacy: the development of mammalian hematopoietic stem cells. *Nature Immunology, 9*, 129–136.
2. Wang, L. D., & Wagers, A. J. (2011). Dynamic niches in the origination and differentiation of haematopoietic stem cells. *Nature Reviews Molecular Cell Biology, 12*, 643–655.
3. Mizuochi, C., Fraser, S. T., Biasch, K., Horio, Y., Kikushige, Y., Tani, K., Akashi, K., Tavian, M., & Sugiyama, D. (2012). Intra-aortic clusters undergo endothelial to hematopoietic phenotypic transition during early embryogenesis. *PLoS One*; in press.
4. Sasaki, T., Mizuochi, C., Horio, Y., Nakao, K., Akashi, K., & Sugiyama, D. (2010). Regulation of hematopoietic cell clusters in the placental niche through SCF/Kit signaling in embryonic mouse. *Development, 137*, 3941–3952.
5. Sugiyama, D., Kulkeaw, K., Mizuochi, C., Horio, Y., & Okayama, S. (2011). Hepatoblasts comprise a niche for fetal liver erythropoiesis through cytokine production. *Biochemical and Biophysical Research Communications, 410*, 301–306.
6. Sugiyama, D., Inoue-Yokoo, T., Fraser, S. T., Kulkeaw, K., Mizuochi, C., & Horio, Y. (2011). Embryonic regulation of the mouse hematopoietic niche. *Scientific World Journal, 11*, 1770–1780.
7. Evans, M. J., & Kaufman, M. H. (1981). Establishment in culture of pluripotential cells from mouse embryos. *Nature, 292*, 154–156.
8. Takahashi, K., & Yamanaka, S. (2006). Induction of pluripotent stem cells from mouse embryonic and adult fibroblast cultures by defined factors. *Cell, 126*, 663–676.
9. Orr-Urtreger, A., Bedford, M. T., Do, M. S., Eisenbach, L., & Lonai, P. (1992). Developmental expression of the alpha receptor for platelet-derived growth factor, which is deleted in the embryonic lethal Patch mutation. *Development, 115*, 289–303.
10. Takakura, N., Yoshida, H., Ogura, Y., Kataoka, H., & Nishikawa, S. (1997). PDGFR alpha expression during mouse embryogenesis: immunolocalization analyzed by whole-mount immunohistostaining using the monoclonal anti-mouse PDGFR alpha antibody APA5. *Journal of Histochemistry and Cytochemistry, 45*, 883–893.
11. Kabrun, N., Buhring, H. J., Choi, K., Ullrich, A., Risau, W., & Keller, G. (1997). Flk-1 expression defines a population of early embryonic hematopoietic precursors. *Development, 124*, 2039–2048.
12. Choi, K., Kennedy, M., Kazarov, A., Papadimitriou, J. C., & Keller, G. (1998). A common precursor for hematopoietic and endothelial cells. *Development, 125*, 725–732.
13. Fehling, H. J., Lacaud, G., Kubo, A., et al. (2003). Tracking mesoderm induction and its specification to the hemangioblast during embryonic stem cell differentiation. *Development, 130*, 4217–4227.
14. Sakurai, H., Era, T., Jakt, L. M., Okada, M., Nakai, S., & Nishikawa, S. (2006). In vitro modeling of paraxial and lateral mesoderm differentiation reveals early reversibility. *Stem Cells, 24*, 575–586.
15. Kulkeaw, K., Horio, Y., Mizuochi, C., Ogawa, M., & Sugiyama, D. (2010). Variation in hematopoietic potential of induced pluripotent stem cell lines. *Stem Cell Reviews, 6*, 381–389.
16. Inoue, T., Kulkeaw, K., Okayama, S., Tani, K., & Sugiyama, D. (2011). Variation in mesodermal and hematopoietic potential of adult skin-derived induced pluripotent stem cell lines in mice. *Stem Cell Reviews, 7*, 958–968.
17. Niwa, A., Heike, T., Umeda, K., et al. (2011). A novel serum-free monolayer culture for orderly hematopoietic differentiation of human pluripotent cells via mesodermal progenitors. *PLoS One, 6*, e22261.
18. Morishima, T., Watanabe, K., Niwa, A., et al. (2011). Neutrophil differentiation from human-induced pluripotent stem cells. *Journal of Cellular Physiology, 226*, 1283–1291.
19. Grigoriadis, A. E., Kennedy, M., Bozec, A., et al. (2010). Directed differentiation of hematopoietic precursors and functional osteoclasts from human ES and iPS cells. *Blood, 115*, 2769–2776.
20. Tolar, J., Park, I. H., Xia, L., et al. (2011). Hematopoietic differentiation of induced pluripotent stem cells from patients with mucopolysaccharidosis type I (Hurler syndrome). *Blood, 117*, 839–847.
21. Burt, R. K., Verda, L., Kim, D. A., Oyama, Y., Luo, K., & Link, C. (2004). Embryonic stem cells as an alternate marrow donor source: engraftment without graft-versus-host disease. *The Journal of Experimental Medicine, 199*, 895–904.
22. Kyba, M., Perlingeiro, R. C., & Daley, G. Q. (2002). HoxB4 confers definitive lymphoid-myeloid engraftment potential on embryonic stem cell and yolk sac hematopoietic progenitors. *Cell, 109*, 29–37.
23. Wang, Y., Yates, F., Naveiras, O., Ernst, P., & Daley, G. Q. (2005). Embryonic stem cell-derived hematopoietic stem cells. *Proceedings of the National Academy of Sciences of the United States of America, 102*, 19081–19086.
24. Zhang, X. B., Beard, B. C., Trobridge, G. D., et al. (2008). High incidence of leukemia in large animals after stem cell gene therapy with a HOXB4-expressing retroviral vector. *The Journal of Clinical Investigation, 118*, 1502–1510.
25. Hanna, J., Wernig, M., Markoulaki, S., et al. (2007). Treatment of sickle cell anemia mouse model with iPS cells generated from autologous skin. *Science, 318*, 1920–1923.
26. Lin, J., Fernandez, I., & Roy, K. (2011). Development of feeder-free culture systems for generation of ckit+sca1+ progenitors from mouse iPS cells. *Stem Cell Reviews, 7*, 736–747.
27. Wang, L., Menendez, P., Shojaei, F., et al. (2005). Generation of hematopoietic repopulating cells from human embryonic stem

cells independent of ectopic HOXB4 expression. *The Journal of Experimental Medicine, 201*, 1603–1614.
28. Nakano, T., Kodama, H., & Honjo, T. (1994). Generation of lymphohematopoietic cells from embryonic stem cells in culture. *Science, 265*, 1098–1101.
29. Nakano, T., Kodama, H., & Honjo, T. (1996). In vitro development of primitive and definitive erythrocytes from different precursors. *Science, 272*, 722–724.
30. Motoyama, N., Kimura, T., Takahashi, T., Watanabe, T., & Nakano, T. (1999). bcl-x prevents apoptotic cell death of both primitive and definitive erythrocytes at the end of maturation. *The Journal of Experimental Medicine, 189*, 1691–1698.
31. Keller, G., Kennedy, M., Papayannopoulou, T., & Wiles, M. V. (1993). Hematopoietic commitment during embryonic stem cell differentiation in culture. *Molecular and Cellular Biology, 13*, 473–486.
32. Carotta, S., Pilat, S., Mairhofer, A., et al. (2004). Directed differentiation and mass cultivation of pure erythroid progenitors from mouse embryonic stem cells. *Blood, 104*, 1873–1880.
33. Ma, F., Ebihara, Y., Umeda, K., et al. (2008). Generation of functional erythrocytes from human embryonic stem cell-derived definitive hematopoiesis. *Proceedings of the National Academy of Sciences of the United States of America, 105*, 13087–13092.
34. Lu, S. J., Feng, Q., Park, J. S., et al. (2008). Biologic properties and enucleation of red blood cells from human embryonic stem cells. *Blood, 112*, 4475–4484.
35. Lengerke, C., Grauer, M., Niebuhr, N. I., et al. (2009). Hematopoietic development from human induced pluripotent stem cells. *Annals of the New York Academy of Sciences, 1176*, 219–227.
36. Raya, A., Rodriguez-Piza, I., Guenechea, G., et al. (2009). Disease-corrected haematopoietic progenitors from Fanconi anaemia induced pluripotent stem cells. *Nature, 460*, 53–59.
37. Ye, Z., Zhan, H., Mali, P., et al. (2009). Human-induced pluripotent stem cells from blood cells of healthy donors and patients with acquired blood disorders. *Blood, 114*, 5473–5480.
38. Era, T., Takagi, T., Takahashi, T., Bories, J. C., & Nakano, T. (2000). Characterization of hematopoietic lineage-specific gene expression by ES cell in vitro differentiation induction system. *Blood, 95*, 870–878.
39. Eto, K., Murphy, R., Kerrigan, S. W., et al. (2002). Megakaryocytes derived from embryonic stem cells implicate CalDAG-GEFI in integrin signaling. *Proceedings of the National Academy of Sciences of the United States of America, 99*, 12819–12824.
40. Fujimoto, T. T., Kohata, S., Suzuki, H., Miyazaki, H., & Fujimura, K. (2003). Production of functional platelets by differentiated embryonic stem (ES) cells in vitro. *Blood, 102*, 4044–4051.
41. Kaufman, D. S., Hanson, E. T., Lewis, R. L., Auerbach, R., & Thomson, J. A. (2001). Hematopoietic colony-forming cells derived from human embryonic stem cells. *Proceedings of the National Academy of Sciences of the United States of America, 98*, 10716–10721.
42. Gaur, M., Kamata, T., Wang, S., Moran, B., Shattil, S. J., & Leavitt, A. D. (2006). Megakaryocytes derived from human embryonic stem cells: a genetically tractable system to study megakaryocytopoiesis and integrin function. *Journal of Thrombosis and Haemostasis, 4*, 436–442.
43. Takayama, N., Nishikii, H., Usui, J., et al. (2008). Generation of functional platelets from human embryonic stem cells in vitro via ES-sacs, VEGF-promoted structures that concentrate hematopoietic progenitors. *Blood, 111*, 5298–5306.
44. Takayama, N., Nishimura, S., Nakamura, S., et al. (2010). Transient activation of c-MYC expression is critical for efficient platelet generation from human induced pluripotent stem cells. *The Journal of Experimental Medicine, 207*, 2817–2830.
45. Wiles, M. V., & Keller, G. (1991). Multiple hematopoietic lineages develop from embryonic stem (ES) cells in culture. *Development, 111*, 259–267.
46. Lindmark, H., Rosengren, B., Hurt-Camejo, E., & Bruder, C. E. (2004). Gene expression profiling shows that macrophages derived from mouse embryonic stem cells is an improved in vitro model for studies of vascular disease. *Experimental Cell Research, 300*, 335–344.
47. Moore, K. J., Fabunmi, R. P., Andersson, L. P., & Freeman, M. W. (1998). In vitro-differentiated embryonic stem cell macrophages: a model system for studying atherosclerosis-associated macrophage functions. *Arteriosclerosis, Thrombosis, and Vascular Biology, 18*, 1647–1654.
48. Senju, S., Haruta, M., Matsunaga, Y., et al. (2009). Characterization of dendritic cells and macrophages generated by directed differentiation from mouse induced pluripotent stem cells. *Stem Cells, 27*, 1021–1031.
49. Lieber, J. G., Webb, S., Suratt, B. T., et al. (2004). The in vitro production and characterization of neutrophils from embryonic stem cells. *Blood, 103*, 852–859.
50. Yokoyama, Y., Suzuki, T., Sakata-Yanagimoto, M., et al. (2009). Derivation of functional mature neutrophils from human embryonic stem cells. *Blood, 113*, 6584–6592.
51. Saeki, K., Nakahara, M., Matsuyama, S., et al. (2009). A feeder-free and efficient production of functional neutrophils from human embryonic stem cells. *Stem Cells, 27*, 59–67.
52. Choi, K. D., Vodyanik, M. A., & Slukvin, I. I. (2009). Generation of mature human myelomonocytic cells through expansion and differentiation of pluripotent stem cell-derived lin-CD34+CD43+CD45+ progenitors. *The Journal of Clinical Investigation, 119*, 2818–2829.
53. Zou, J., Sweeney, C. L., Chou, B. K., et al. (2011). Oxidase-deficient neutrophils from X-linked chronic granulomatous disease iPS cells: functional correction by zinc finger nuclease-mediated safe harbor targeting. *Blood, 117*, 5561–5572.
54. Cho, S. K., Webber, T. D., Carlyle, J. R., Nakano, T., Lewis, S. M., & Zuniga-Pflucker, J. C. (1999). Functional characterization of B lymphocytes generated in vitro from embryonic stem cells. *Proceedings of the National Academy of Sciences of the United States of America, 96*, 9797–9802.
55. Wada, H., Kojo, S., Kusama, C., et al. (2011). Successful differentiation to T cells, but unsuccessful B-cell generation, from B-cell-derived induced pluripotent stem cells. *International Immunology, 23*, 65–74.
56. Vodyanik, M. A., Bork, J. A., Thomson, J. A., & Slukvin, I. I. (2005). Human embryonic stem cell-derived CD34+ cells: efficient production in the coculture with OP9 stromal cells and analysis of lymphohematopoietic potential. *Blood, 105*, 617–626.
57. Carpenter, L., Malladi, R., Yang, C. T., et al. (2011). Human induced pluripotent stem cells are capable of B-cell lymphopoiesis. *Blood, 117, 4008–4011.*
58. de Pooter, R. F., Cho, S. K., Carlyle, J. R., & Zuniga-Pflucker, J. C. (2003). In vitro generation of T lymphocytes from embryonic stem cell-derived prehematopoietic progenitors. *Blood, 102*, 1649–1653.
59. Schmitt, T. M., de Pooter, R. F., Gronski, M. A., Cho, S. K., Ohashi, P. S., & Zuniga-Pflucker, J. C. (2004). Induction of T cell development and establishment of T cell competence from embryonic stem cells differentiated in vitro. *Nature Immunology, 5*, 410–417.
60. Lei, F., Haque, R., Weiler, L., Vrana, K. E., & Song, J. (2009). T lineage differentiation from induced pluripotent stem cells. *Cellular Immunology, 260*, 1–5.
61. Galic, Z., Kitchen, S. G., Kacena, A., et al. (2006). T lineage differentiation from human embryonic stem cells. *Proceedings of the National Academy of Sciences of the United States of America, 103*, 11742–11747.
62. Galic, Z., Kitchen, S. G., Subramanian, A., et al. (2009). Generation of T lineage cells from human embryonic stem cells in a feeder free system. *Stem Cells, 27*, 100–107.
63. Timmermans, F., Velghe, I., Vanwalleghem, L., et al. (2009). Generation of T cells from human embryonic stem cell-derived hematopoietic zones. *Journal of Immunology, 182*, 6879–6888.
64. Martin, C. H., Woll, P. S., Ni, Z., Zuniga-Pflucker, J. C., & Kaufman, D. S. (2008). Differences in lymphocyte developmental potential

between human embryonic stem cell and umbilical cord blood-derived hematopoietic progenitor cells. *Blood, 112*, 2730–2737.
65. Lian, R. H., Maeda, M., Lohwasser, S., et al. (2002). Orderly and nonstochastic acquisition of CD94/NKG2 receptors by developing NK cells derived from embryonic stem cells in vitro. *Journal of Immunology, 168*, 4980–4987.
66. Watarai, H., Fujii, S., Yamada, D., et al. (2010). Murine induced pluripotent stem cells can be derived from and differentiate into natural killer T cells. *The Journal of Clinical Investigation, 120*, 2610–2618.
67. Ni, Z., Knorr, D. A., Clouser, C. L., et al. (2011). Human pluripotent stem cells produce natural killer cells that mediate anti-HIV-1 activity by utilizing diverse cellular mechanisms. *Journal of Virology, 85*, 43–50.
68. Szabo, E., Rampalli, S., Risueno, R. M., et al. (2010). Direct conversion of human fibroblasts to multilineage blood progenitors. *Nature, 468, 521–526.*